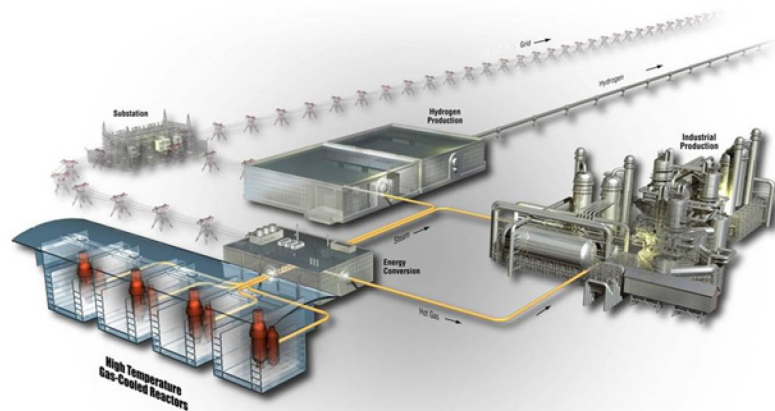




# RELAP5-3D Simulation of PG-27 Test at the HTTF Facility.

September 2021

Abhinav Gairola  
Aaron S. Epiney



#### **DISCLAIMER**

This information was prepared as an account of work sponsored by an agency of the U.S. Government. Neither the U.S. Government nor any agency thereof, nor any of their employees, makes any warranty, expressed or implied, or assumes any legal liability or responsibility for the accuracy, completeness, or usefulness, of any information, apparatus, product, or process disclosed, or represents that its use would not infringe privately owned rights. References herein to any specific commercial product, process, or service by trade name, trade mark, manufacturer, or otherwise, does not necessarily constitute or imply its endorsement, recommendation, or favoring by the U.S. Government or any agency thereof. The views and opinions of authors expressed herein do not necessarily state or reflect those of the U.S. Government or any agency thereof.

# **RELAP5-3D Simulation of PG-27 Test at the HTTF Facility**

**Abhinav Gairola**  
**Aaron S. Epiney**

**September 2021**

**Idaho National Laboratory**  
**Idaho Falls, Idaho 83415**

**<http://www.ART.INL.gov>**

**Prepared for the**  
**U.S. Department of Energy**  
**Office of Nuclear Energy**  
**Under DOE Idaho Operations Office**  
**Contract DE-AC07-05ID14517**

*Page intentionally left blank*

**INL ART Program**  
**RELAP5-3D Simulation of PG-27 Test at the HTTF**  
**Facility**

INL/EXT-21-63798  
Revision 0

**September 2021**

**Technical Reviewer:** (Confirmation of mathematical accuracy, and correctness of data and appropriateness of assumptions.)

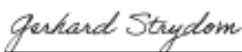


\_\_\_\_\_  
Paolo Balestra  
HTGR Methods Lead

Aug 3 2021

\_\_\_\_\_  
Date

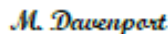
**Approved by:**



\_\_\_\_\_  
Gerhard Strydom  
ART Co-National Technical Director

08/03/2021

\_\_\_\_\_  
Date



\_\_\_\_\_  
Michael E. Davenport  
ART Project Manager

8/3/21

\_\_\_\_\_  
Date



\_\_\_\_\_  
Michelle T. Sharp  
INL Quality Assurance

8/2/21

\_\_\_\_\_  
Date



## **ABSTRACT**

The High Temperature Test Facility (HTTF) at Oregon State University (OSU) is a quarter-scaled integral-effect test facility designed to examine the transient phenomena occurring in a Modular High-Temperature Gas-cooled Reactor (MHTGR). It is specifically designed to handle the Pressurized Conduction Cooldown (PCC) and Depressurized Conduction Cooldown (DCC) events. The PCC event is an accident scenario in which there is a loss of the forced convection of the coolant through the system. However, the pressure boundary remains intact. This study focuses on the Reactor Excursions and Leak Analysis Program (RELAP5-3D) simulation of the PG-27 test (PCC phenomena) and the sensitivity of those simulations from the material properties and primary helium mass flow rate standpoint. The aim is to capture a reasonable 1D picture of a 3D phenomena. The simulation will help in the code assessment and in understanding the various unknown parameters involved. The presented results will demonstrate that the code is able to capture the detailed 1D physics accurately. However, input parameters to the code (i.e., the primary mass flow rate, refractory material thermal conductivity, and heat capacity at elevated temperatures) impact the fuel temperature the most. This work will discuss the sensitivity of simulations to the identified input parameters.

*Page intentionally left blank*



## CONTENTS

ABSTRACT.....	3
ACRONYMS.....	8
1. INTRODUCTION.....	10
2. HIGH TEMPERATURE TEST FACILITY .....	11
2.1 Types of Instrumentation .....	12
3. PG-27 TEST DESCRIPTION.....	13
3.1 Initial Conditions.....	13
3.2 Input Power .....	14
3.3 Reactor Cavity Cooling System .....	15
3.4 Steam Generator Performance .....	15
3.5 Primary Pump Speed.....	16
4. INPUT MODEL DESCRIPTION .....	16
4.1 RELAP5-3D HTTF Model .....	16
5. RELAP5-3D SIMULATION SETUP AND INPUT DATA PROCESSING .....	17
5.1 Helium Mass Flow Rate.....	18
6. RESULTS .....	22
6.1 Conclusion .....	28

## FIGURES

Figure 1. HTTF primary pressure vessel (right), Reactor Cavity Simulation Tank (RCST), and hot and cold ducts. ....	11
Figure 2. Major instruments in HTTF and their counts. ....	12
Figure 3. Correct initial conditions are very important for the right evolution of the experimental and numerical transients. ....	13
Figure 4. Measured heater output in heater Bank Number 102 and 108. ....	14
Figure 5. Normalized (0-1) variables representing the RCCS operation. ....	15
Figure 6. Normalized (0-1) variables representing the steam generator operation. ....	15
Figure 7. Primary circulator speed vs temperature in the core. Here the blue vertical line shows the time at which the transient begins.....	16
Figure 8. RELAP5-3D nodalization of the HTTF facility. ....	17
Figure 9. Mass flow rate computed via energy balance at dominant pump speeds (Circulator inlet temperature in green and circulator outlet temperature in red. The circulator is cooled, which explained the drop in temperature over the circulator).....	19

Figure 10. Dominant pump speeds. ....	20
Figure 11. Head vs. mass flow rate at 100% speed. The extrapolated curve to accounts for those flow rates that were missing in the supplied data. ....	21
Figure 12. Statistical analysis of the pressure vs. pump speeds at various dominant pump speeds. The pressure is never settling to one single value. ....	21
Figure 13. Statistical variation of temperature in Core Block #3 and Primary Sector #5 owing to the variation in the flow rate. The bands show $\mu \pm 2 \times \sigma$ . ....	23
Figure 14. Statistical variation of the temperature in Core Block #3 and Pprimary Sector #5 owing to the variation in the conductivity. The bands show $\mu \pm 2 \times \sigma$ .....	24
Figure 15. Temperature distribution (in Kelvin) in Core Block #1. ....	26
Figure 16. Temperature distribution (in Kelvin) in Core Block #3. ....	27

## TABLES

Table 1. Initial conditions. ....	14
Table 2. Helium mass flow rate computed via energy balance. The negative mass flow rate at 30% pump speed is not possible; further the flow rate computed at higher pump speeds is too high to be trustworthy. ....	18
Table 3. Computed base helium mass flow rates using the head vs mass flow rate curves.....	22
Table 4. Sensor locations in Core Block # 1.....	24
Table 5. Sensor locations in Core Block # 3.....	25

*Page intentionally left blank*

## ACRONYMS

DCC	Depressurized Conduction Cooldown
HTGR	High-Temperature Gas-cooled Reactor
HTTF	High Temperature Test Facility
INL	Idaho National Laboratory
MHTGR	Modular High-Temperature Gas-cooled Reactor
OSU	Oregon State University
PCC	Pressurized Conduction Cooldown
PCS	Primary Coolant System
PHISICS	Parallel and Highly Innovative Simulation for INL Code System
RCCS	Reactor Cavity Cooling System
RCST	Reactor Cavity Simulation Tank
RELAP	Reactor Excursions and Leak Analysis Program
SCS	Secondary Cooling System

*Page intentionally left blank*

# 1. INTRODUCTION

The computer model of a physical plant provides valuable insight into the behavior of an engineered physical system at both the operating point and beyond. These computer models often come in the form of an executable code that relies on differential equations for analyzing the system. The underlying governing equations to the code are a numerical representation of the system under consideration, which of course comes with certain approximations. Owing to these approximations, there is a possibility that they may not be free from modeling deficiencies. Therefore, validation (i.e. comparing the analytical results obtained by the code with the experimental data) and verification (i.e. performing sanity checks that it meets its design specifications by comparing coding to algorithms and equations and comparing calculations against analytical solutions and method of manufactured solutions.) (Mesina, Aumiller, and Buschman 2016) of the numerical models and schemes become an important part of the code development process.

Reactor Excursions and Leak Analysis Program (RELAP5-3D) is one such computational thermal-hydraulics code designed for the safety analysis of the nuclear systems. It is an offshoot of the RELAP5 code development program which was originally designed for the analysis of pressurized-water reactors. The objective of the RELAP5-3D program was to provide the various stakeholders and users an analytical tool for the independent evaluation of both nuclear and non-nuclear systems.

The latest iteration of the code builds significantly over its predecessors, as it incorporates variable gravity to model moving systems, NESTLE for multidimensional neutronics with nodal kinetics, coupling with the Parallel and Highly Innovative Simulation for INL Code System (PHISICS) for massively parallel neutron kinetics, one and two-dimensional heat transfer including conduction, convection, and radiation and gas diffusion, radiological transport, and alternate heat conduction to the fluid. These additions remove any restrictions on the applicability of the code to the full range of postulated reactor accidents (Uspuras, Kaliatka, and Bubelis 2004) and (Mesina 2016). However, before performing any real-life calculation with a code it must be validated, which requires conducting experiments. Experiments are needed as they provide confidence in the postulation and hypothesis posed during the numerical model development phase. Over the years, the RELAP5-3D has been validated against various experimental benchmarks for light-water reactors and the physics has been proven. For the high temperature-gas (Davis 2018) and liquid metal (Novo and Martelli 2016) applications, validation it is an ongoing effort and is quintessential in the development of Generation-IV reactor technology.

The Modular High-Temperature Gas-cooled Reactor (MHTGR) is an advanced high-temperature gas reactor designed by General Atomics, which retains basic High-Temperature Gas-cooled Reactor (HTGR) (Gen IV) features of ceramic fuel, helium coolant, and graphite. It is sized and configured to provide a low power density core with passive safety features such that no operator action or external source of power is needed for the plant (Neylan, Graf, and Millunzi 1988). The performance of advanced passive safety feature needs to be assessed before a full-blown production of the system is done.

To this end, a quarter-scaled integral-effect test facility (named the High Temperature Test Facility or HTTF) of an MHTGR was designed and built at Oregon State University (OSU). The data generated by this facility has been used in the past to validate the Depressurized Conduction Cooldown (DCC) mode of heat transfer (Epiney 2020). This report deals with the simulation of a Pressurized Conduction Cooldown (PCC) test called PG-27. An overview of the test facility is provided in the next section, followed by a description of HTTF test PG-27.

## 2. HIGH TEMPERATURE TEST FACILITY

The HTTF is a helium-cooled, electrically heated integral experiment facility of the General Atomics MHTGR. It uses prismatic graphite blocks in the core and reflectors. Its pressure vessel and core are scaled by one-quarter diametrically and axially. Most of the coolant channels in the core are full scale, with smaller diameter channels around the core periphery. The facility operates at low pressure, compared to the prototype reactor, and primarily investigates DCC and PCC transients (see Figure 1).

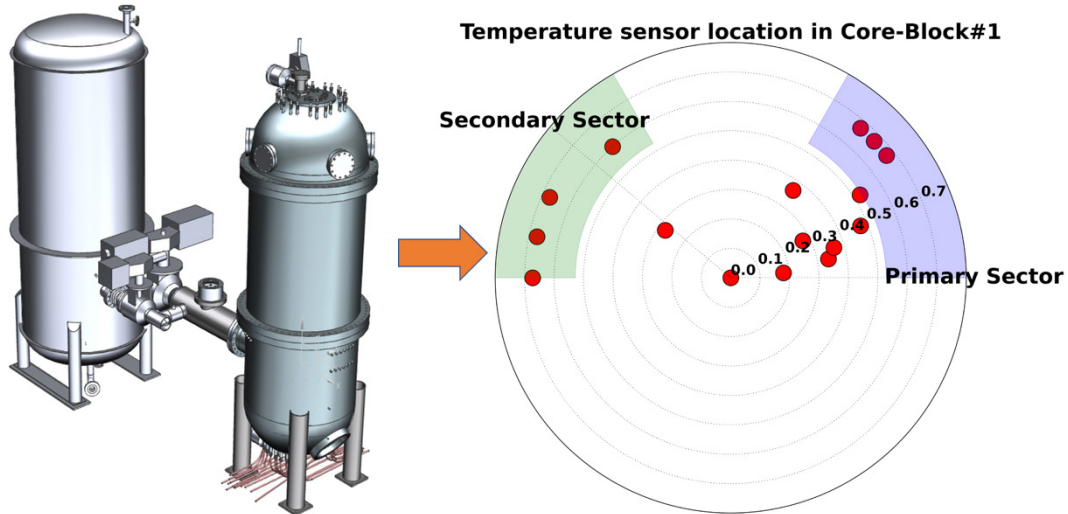


Figure 1. HTTF primary pressure vessel (right), Reactor Cavity Simulation Tank (RCST), and hot and cold ducts.

The facility is described in detail in Brian Woods’ “OSU High Temperature Test Facility Technical Design Report” (Woods 2019) and includes several systems. The primary coolant system (PCS) has a pressure vessel, a concentric hot and cold duct, a steam generator, a gas circulator, and connecting pipes. Break valves in both the hot and cold legs connect to a large RCST, whose gas composition can be initialized to a range of values to simulate the different conditions that may exist outside the reactor vessel following a loss-of-coolant accident.

Alumina ceramic blocks are used to simulate the core and the top and bottom reflectors. Each block encompasses the radial region occupied by the central reflector, fuel, and side reflector in the MHTGR. Holes in the blocks provide channels for the heater rods, which consist of stacks of graphite rodlets. The rods are grouped into ten heater banks, each of which contains 21 heater rods. Smaller coolant holes are arranged in a hexagonal pattern around the heater rods. Larger holes cast in the central and side reflector regions represent the core bypass flow in these regions. Permanent or outer reflector blocks, made of a different ceramic material, are located between the core blocks and the core barrel. A graphite plate in the upper plenum covers the gaps on either side of the permanent reflector blocks so that the only flow through the core is in the holes cast in the core blocks.

The steam generator has 188 U-tubes. Feedwater is pumped from a supply tank into the downcomer on the secondary side, and any steam generated is vented to the atmosphere.

The principal feature of the Reactor Cavity Cooling System (RCCS) is the cooling panels that surround the pressure vessel. Water flowing through the panels provides the heat sink for the PCS during

most transients. Water is pumped from the same tank as the steam generator feedwater but is recirculated back to the tank after exiting the top of the cooling panels. The inlet flow can be controlled to provide a desired panel outlet temperature, and isolation valves on the panels can be closed to simulate a degraded heat sink.

## 2.1 Types of Instrumentation

The HTTF facility is equipped with a variety of instruments to monitor the evolution of temperature, pressure, fluid levels and power within the HTTF facility (see Figure 2 ). This includes voltage and current transmitters to reconstruct the input power profiles, temperature transmitters to monitor the solid and gas temperatures in a variety of locations. These locations are located at various azimuthal, radial, and axial locations of the core (see Figure 1). The spread of the sensors allows the facility to track and monitor the principle variables (i.e. temperature and pressure) in a multidimensional fashion.

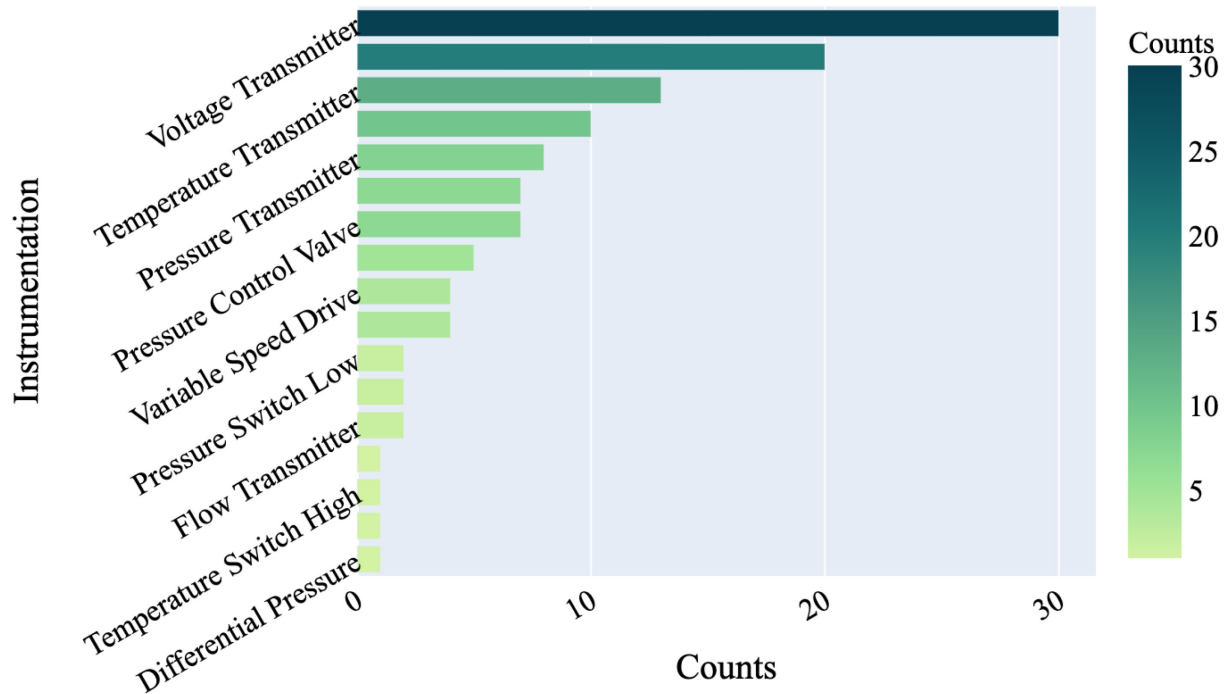


Figure 2. Major instruments in HTTF and their counts.



### 3. PG-27 TEST DESCRIPTION

The PCC or the PG-27 test began on April 23, 2019 and was completed on May 24, 2019. As mentioned before this test examines the PCC phenomena progression in an integral test facility scaled to the General Atomics MHTGR design. The initial conditions in the test were met using low power ( $<350$  kW) and two heater banks, more details about this can be gleaned from (Woods and Cadell 2019). The test progressed as planned with one particular issue related to the chemical reaction in the ceramic material that changes the electrical resistance in the heating cables. This forced the operators to pause the test momentarily. However, this difficulty was overcome, and the test progressed successfully after this singular event. Since this test lasted over one month, not all gathered data was useful. In this paper only data from the final data set (PG27\_G) will be presented and compared with the RELAP5-3D simulations. This particular data set covers a time period of approximately four days. Initial and boundary conditions of the test are presented in the following sections.

#### 3.1 Initial Conditions

For any physical process to go on a particular trajectory or progression of events it is very important to initialize it from the correct starting point or the initial condition. The PG-27 test is divided into two phases; the heat-up phase and the transient phase. During the heat-up phase, the power in the facility keeps increasing. In other words, this means that the test facility should be subjected to the correct energy content before the actual transient starts. Incorrect initial conditions both in the simulations and experimental setup can be a major source of uncertainty (see Figure 3).

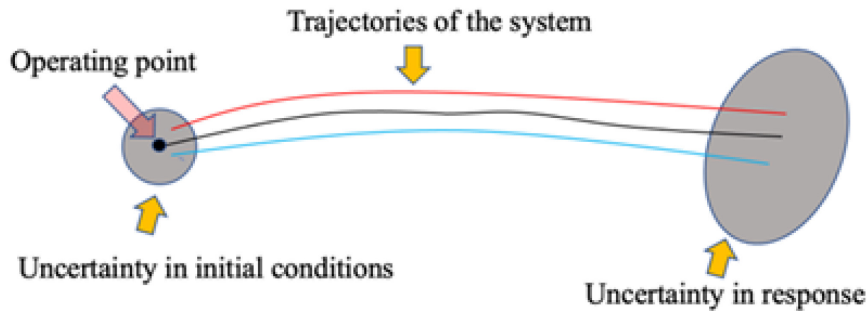


Figure 3. Correct initial conditions are very important for the right evolution of the experimental and numerical transients.

In the current work we modeled both the facility heat up and the actual transient. The initial conditions at the beginning of the heat-up phase are given in Table 1.

Table 1. Initial conditions.

Primary Loop	>130 kPa helium
RCCS	>110 kPa helium
Cooling Water System	Filled with water at ambient pressure and temperature
Steam Generator	60–80% water level at ambient pressure and temperature
RCCS Tank	Filled with water at ambient pressure and temperature
RCCS Panels	Filled with water at ambient pressure and temperature

### 3.2 Input Power

The power input to the test setup is provided by a bank of two heaters. For the PG-27 heater Bank Number 102 and 108 were operated from a starting power of 1kW which reached to a peak power of more than 70kW (see Figure 4 ). Since there isn't a feedback loop for the power control, operators maneuvered the heater power manually. The facility is equipped with voltage (V) and current (C) transmitters. Using the recorded current and voltage measurements the heating power of the heater banks can be computed by the following formula:

$$p_{102} = C_{102} \times V_{102}$$

$$p_{108} = C_{108} \times V_{108}$$

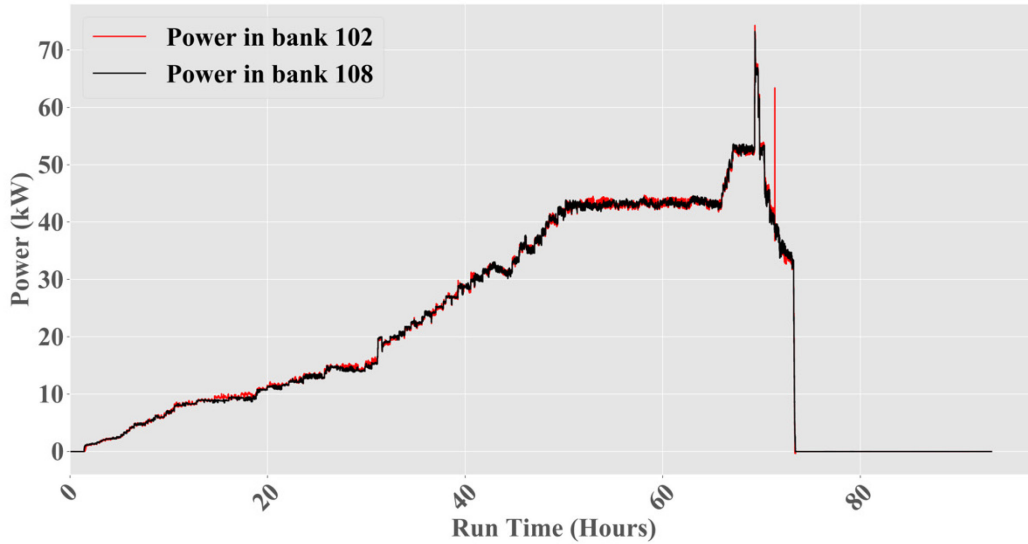


Figure 4. Measured heater output in heater Bank Number 102 and 108.

### 3.3 Reactor Cavity Cooling System

During this test, the RCCS was initially operated when it was filled. It was then operated again during hours 47 and 48 of the test. During hour 66, the RCCS was started and continuously operated until the heaters were secured in hour 73. Thus, it can be concluded that this is not a significant input variable as it is non-operational the majority of time (See Figure 5).

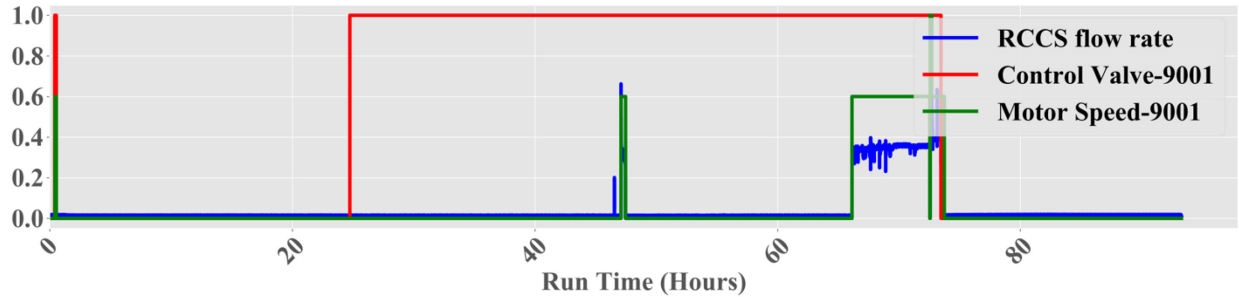


Figure 5. Normalized (0-1) variables representing the RCCS operation.

### 3.4 Steam Generator Performance

During this test, the steam generator was filled to 76% of its volume before the test. Water was added as needed to maintain the level between 60 and 80%. This particular component is not explicitly modeled in the RELAP5-3D model. The effect of the steam generator on the helium temperature and pressure in the primary system is emulated by a boundary condition at the primary outlet of the steam generator (Epiney 2020) (See Figure 6).

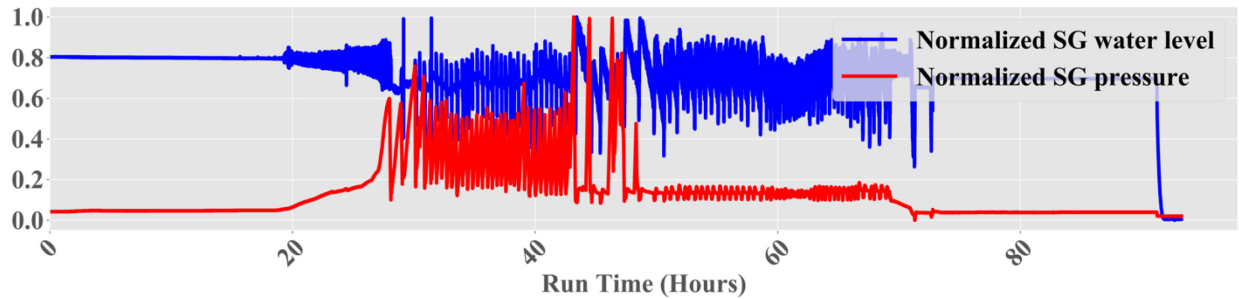


Figure 6. Normalized (0-1) variables representing the steam generator operation.

### 3.5 Primary Pump Speed

During the entire test, the primary pump was maneuvered at different speed levels to control the temperature in the primary side. This variable has significant relationship with the heat transfer (see Figure 7).

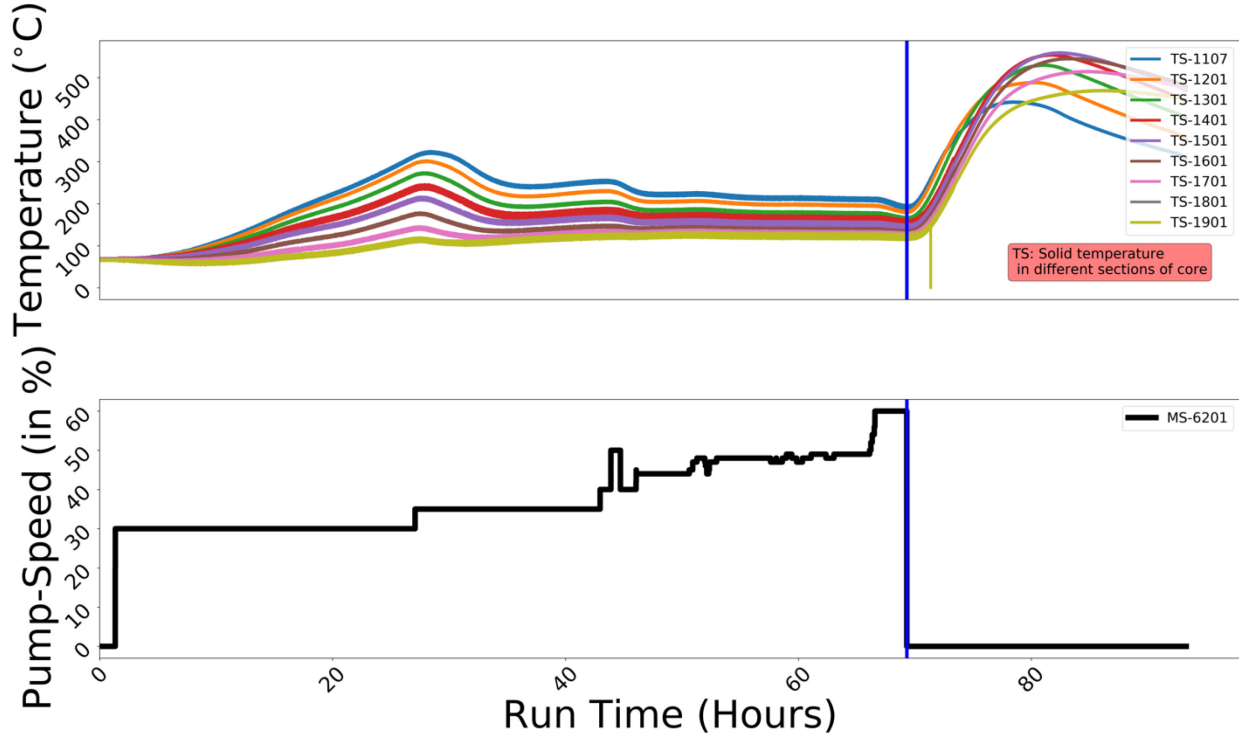


Figure 7. Primary circulator speed vs temperature in the core. Here the blue vertical line shows the time at which the transient begins.

## 4. INPUT MODEL DESCRIPTION

This section briefly describes the RELAP5-3D input model of the HTTF facility.

### 4.1 RELAP5-3D HTTF Model

A quality-controlled RELAP5-3D model of the HTTF facility was developed at Idaho National Laboratory (INL) by Paul D. Bayless (Bayless 2018) and Aaron S. Epiney (Epiney 2020). This model includes hydrodynamic components, heat structures, trips, and control systems to model the various systems of the HTTF facility (i.e. PCS, Secondary Cooling System (SCS), RCCS, and the RCST system). The base quality-controlled model of the HTTF facility was modified by Epiney (Epiney 2020) by splitting and connecting the hot duct hydrodynamic and heat structure components to explore and understand the single-phase counter-current helium flow in a DCC transient. This modified version of the original HTTF model was used in this work to simulate the PG-27 transient. Since RELAP5-3D solves the governing equation in discrete sections of the model geometry, therefore, it is essential to show and discuss the nodalization of the test section (see Figure 8 for details).

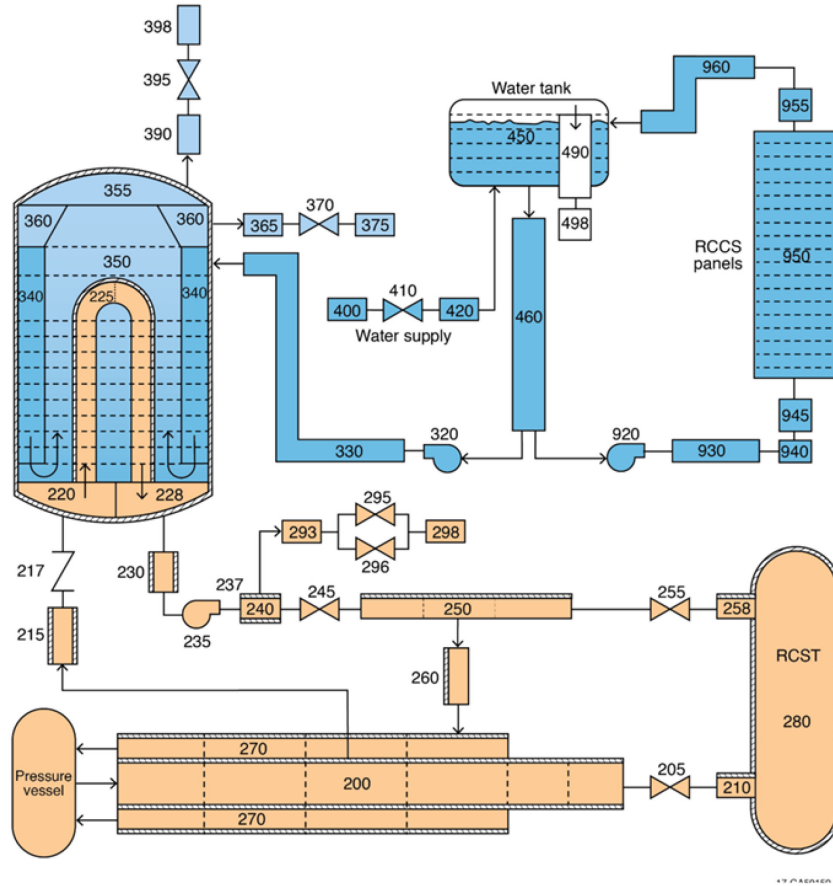


Figure 8. RELAP5-3D nodalization of the HTTF facility.

The most important and noteworthy test section process from the PG-27 transient progression point of view is when the hot gas exits the primary pressure vessel into the modified hot duct (Components 200 and 206), then flows up through a check valve (Component 217) and into the steam generator inlet plenum and tubes (Components 220 and 225). The cooled gas flows out of the steam generator outlet plenum (Component 228) into a piping (Component 230) that leads to the gas circulator. The circulator is modeled using a branch (Component 235) and a time-dependent junction (Component 237). From the circulator, the flow proceeds through an isolation valve (Component 245), into a crossover pipe (Component 260), into an annulus around the hot duct (the cold duct, Component 270), and then back into the primary pressure vessel.

In the core regions, two heat structures were used in each channel. These heat structures model the heater and the ceramic material respectively. The heater in each channel radiates heat to the outer region of the ceramic material. This means that negligible contact is assumed between the two heat structure components.

## 5. RELAP5-3D SIMULATION SETUP AND INPUT DATA PROCESSING

The raw data files provided by OSU mark certain detectors as not working that were used in the previous iteration of the model for the PG-26 simulation. Only working sensors were used to generate initial and boundary conditions. Getting as accurate initial conditions as possible is important because the HTTF facility never reached a true steady state, i.e. one cannot use RELAP5-3D in steady state mode to compute initial conditions and restart into a transient, but must directly start a transient form as good as

possible initial conditions specified directly in the input deck. To save time between tests, new tests were started before the facility completely cooled down, i.e. even at time zero of the test, the facility was still cooling down and not in steady state.

As mentioned previously, the most important variables identified during the exploratory data analysis phase from the point of view of the transient progression are the input power and the circulator speed. The core input power was computed from the voltage and current measurements and is parsed to the RELAP5-3D general table connected to the respective heat structures using an automated Python tool (Epiney 2020). A maximum of 5000 data points (which is the upper limit on the allowed data points) were taken conserving main features of the measured data, like minima, maxima and the time integral. In other words, the measured data points (671,699) are beyond the maximum allowable limit in the RELAP5-3D input deck therefore they must be reduced in number. In this way, the correct amount of energy to apply to the system during the heat-up phase is conserved.

## 5.1 Helium Mass Flow Rate

In the RELAP5-3D input model, the circulator is modeled using a branch and a time-dependent junction component. This setup demands a representative mass flow rate for the gas, however no helium mass flow rates were measured during the test. The helium mass flow rate can be estimated in two ways, either by computing a representative mass flow rate using an energy balance approach over the core  $\dot{q} = \dot{m}c_p\Delta T$  or by using the pump curves to compute the mass flow rate using the pressure drop over the circulator. The first approach may not work as the circulator speed varies over a wide range and it is very difficult to find a steady-state point for the temperature at a particular pump speed (Table 2 and Figure 9).

Table 2. Helium mass flow rate computed via energy balance. The negative mass flow rate at 30% pump speed is not possible; further the flow rate computed at higher pump speeds is too high to be trustworthy.

Pump Speed (%)	Computed Mass Flow Rate of Helium ( $\frac{kg}{s}$ )
30	-0.003002
35	0.061783
40	0.174274
44	0.262947
48	0.431185
49	0.521784
50	0.303247
60	0.599021

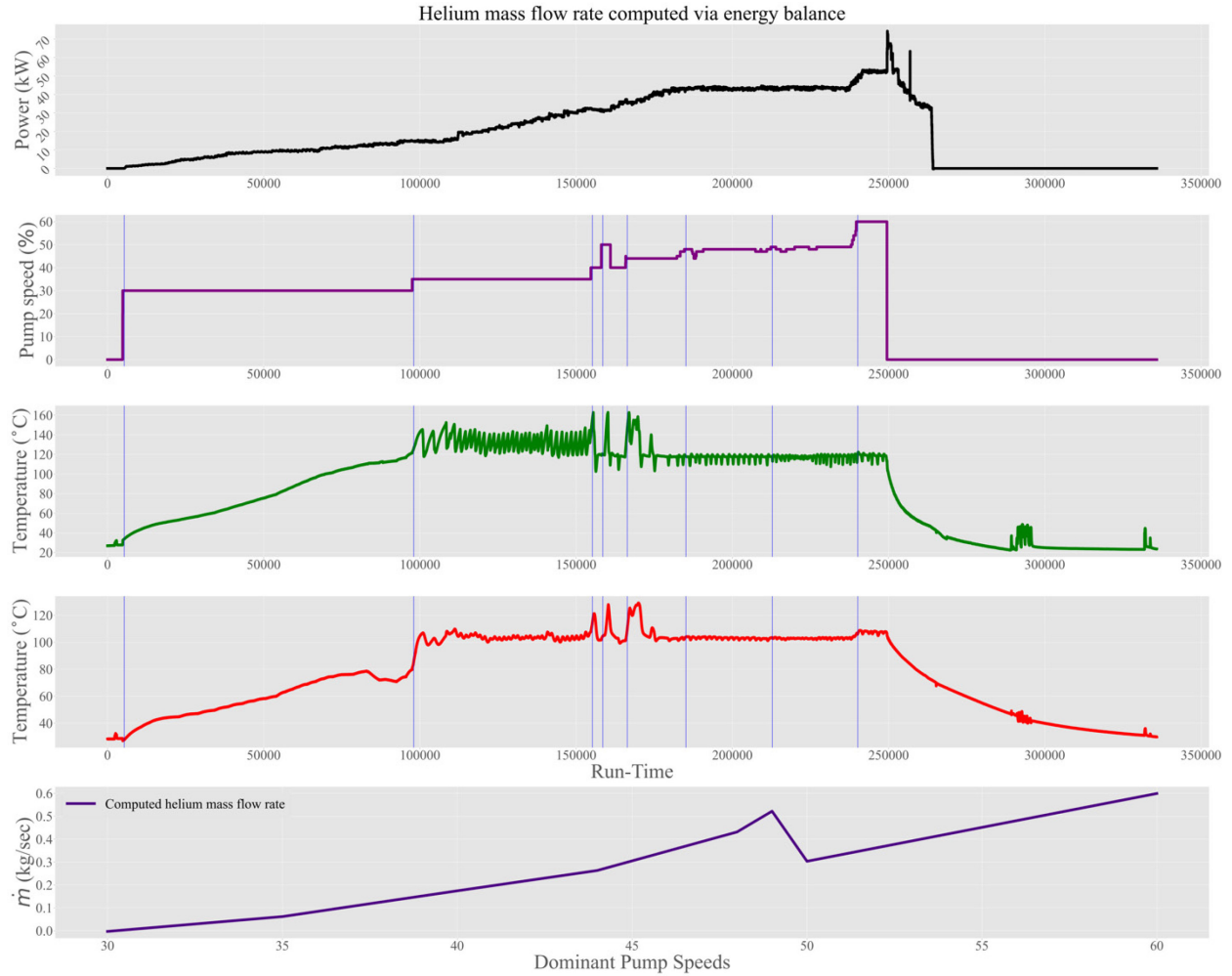


Figure 9. Mass flow rate computed via energy balance at dominant pump speeds (Circulator inlet temperature in green and circulator outlet temperature in red. The circulator is cooled, which explained the drop in temperature over the circulator).

In the second approach, the pressure and the density are determined at a particular speed to compute the mass flow rate. The most dominant speeds were used (see Figure 10). Then, using the head vs. mass flow rate curve (see Figure 11), the pressure is deduced at the rated speed. After this, computing the mass flow rate at the rated or 100% speed and bringing it back to the desired dominant speed is straightforward (Epiney 2020).

Care should be taken when selecting the upper or the lower value (at each pressure the pump curve gives two solutions depending the circulator power consumption; one higher and one lower) of the flow. In Figure 11 (see the red lines), a negative flow rate is observed at 3.5 psig. Not knowing the circulator power during the test, we decided to use the upper points as the flow rate readings.

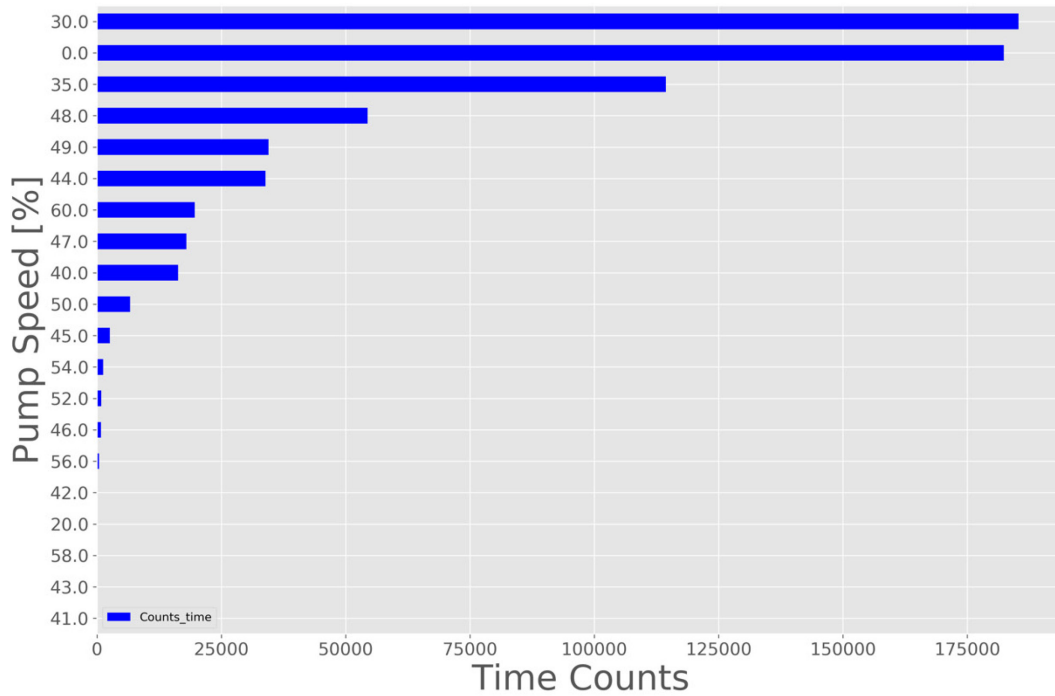


Figure 10. Dominant pump speeds.

The other challenge faced in deducing the correct helium flow rate is the pressure in the test section doesn't remain at a single value and shows very non-stationary behavior (see Figure 12). This leads to the second issue, which pressure value to choose from a list of statistical measures. It was decided to look at the temperature and pressure behavior during the test and select a representative value of the pressure instead of opting for a less trustworthy statistical measure computed by grouping the pressure with the dominant pump speed value. With this estimated pressure value, we computed the pump mass flow rate at the desired dominant pump speed (see Table 3).



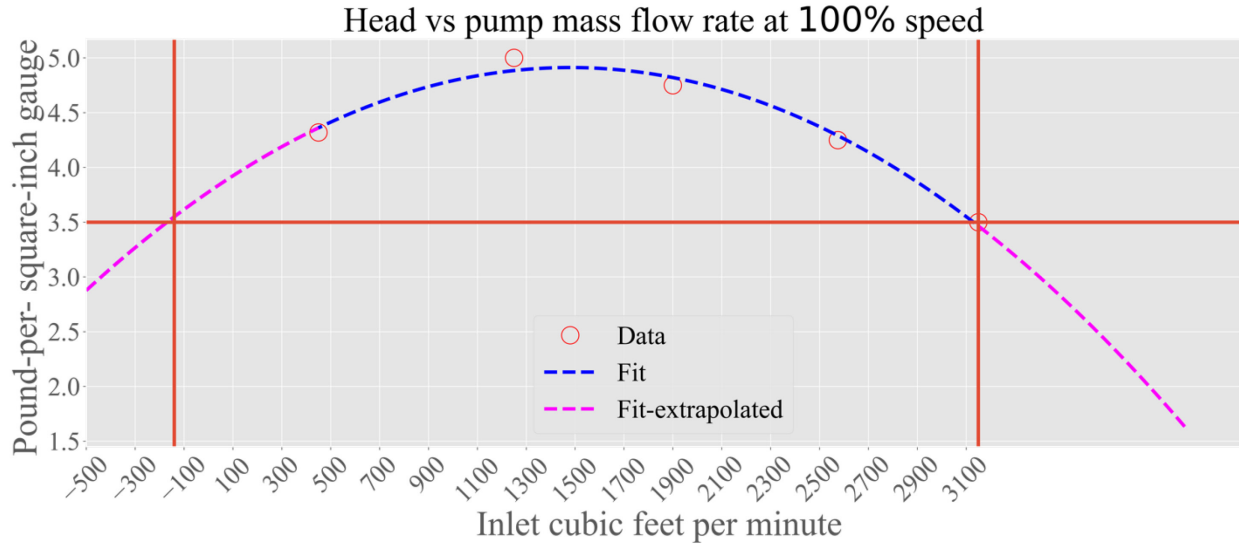


Figure 11. Head vs. mass flow rate at 100% speed. The extrapolated curve to accounts for those flow rates that were missing in the supplied data.

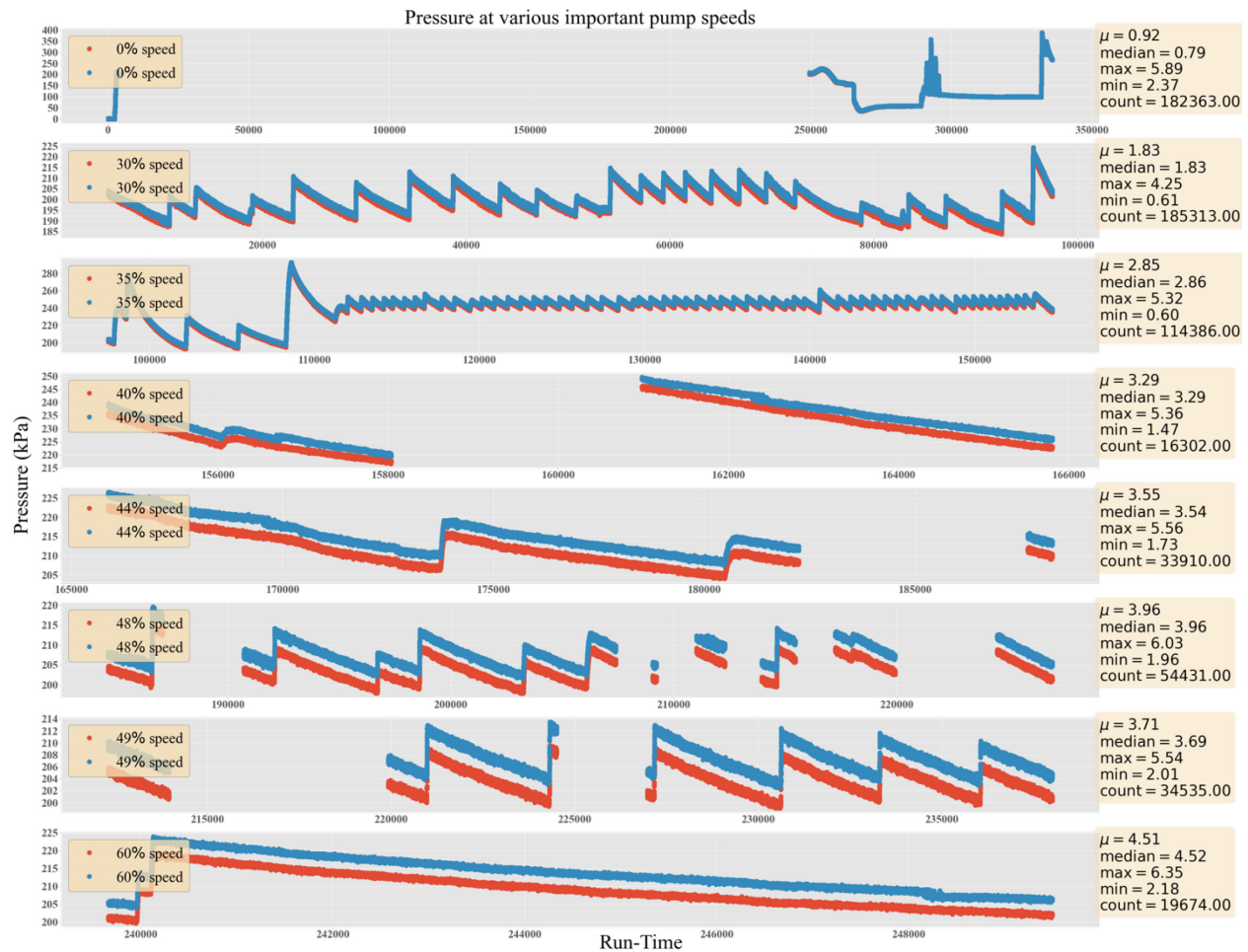


Figure 12. Statistical analysis of the pressure vs. pump speeds at various dominant pump speeds. The pressure is never settling to one single value.

With these values, we created a base RELAP5-3D input case. However, it appears that the computed mass flow rate is on the higher side. Therefore, we decided to perform a sensitivity study on this and to search for an optimal mass flow rate that best predicts measured temperatures. This is achieved by first scaling the flow rate to 30% of the computed mass flow rate and then increasing it to 40, 50, 70, 75, 80 and 90% of the computed base mass flow rate (as shown in Table 3) in the RELAP5-3D input files.

Table 3. Computed base helium mass flow rates using the head vs mass flow rate curves.

Pump Speed (%)	Computed Mass Flow Rate of Helium ( $\frac{kg}{s}$ )
30	0.105
35	0.133
40	0.1665
44	0.194
48	0.215
49	0.22
50	0.226
60	0.285

## 6. RESULTS

The base case (see Figure 13) shows a decent agreement with the overall progression of the transient as described by the comparative line plots tracked in the Core Block #3 and Primary Sector #5—which is the location for measuring the ceramic block temperature.

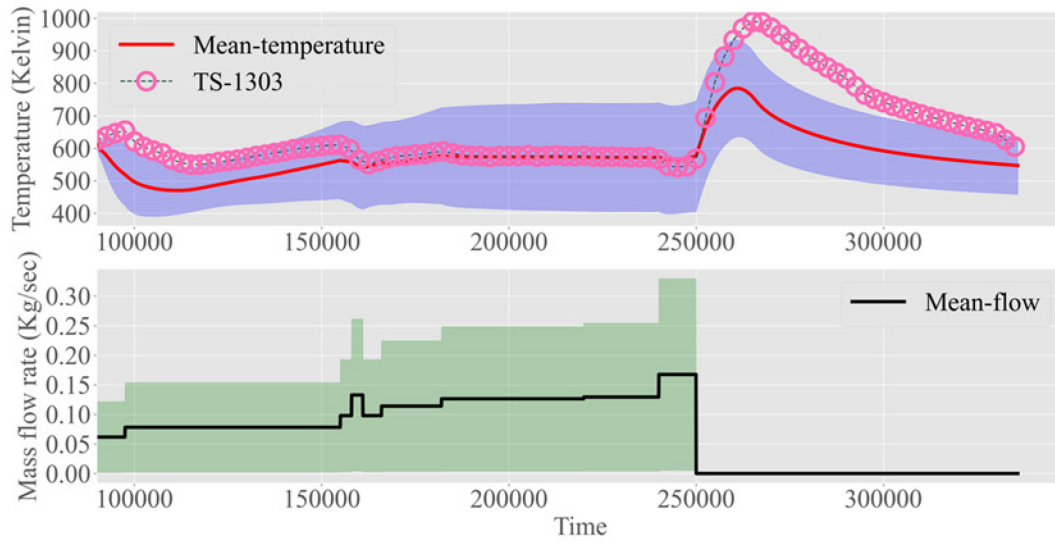


Figure 13. Statistical variation of temperature in Core Block #3 and Primary Sector #5 owing to the variation in the flow rate. The bands show  $\mu \pm 2\sigma$ .

The code was able to simulate the heating of the core and the rise in the solid temperature as soon as the circulator goes offline. However, certain discrepancies are obvious. The heating was not perfectly emulated and the temperature started to go up at around 140,000-time step. This behavior indicates that the supplied flow rate is relatively low. Therefore, the helium mass flow rate was further increased to 80% of the computed base mass flow rate. This correctly emulates the heating of the core. The correct storage of energy into the system during the heating up phase leads to the right progression of the transient later. Nevertheless, the increased helium mass flow rate leads to a suppression of the peak temperature observed during the transient progression while the point where the transient starts is correctly captured by it. In order to understand the effect of conductivity on the response variable, we decided to keep the flow fixed at the base mass flow rate and vary the conductivity. These results are shown in Figure 14. From the visual inspection, it is obvious that the response variable shows more diffusive behavior when the flow rate varies. Therefore, the exact flow rate computation is very important to understand the overall physics of this conduction dominant experiment.

By fixing the flow rate at the base mass flow rate when the conductivity was varied, we obtained the best results at one-tenth of the original value of the conductivity. This reduction in conductivity is rather significant and needs some investigation. A possible reason for such a reduction in the conductivity is perhaps a too high helium mass flow rate.

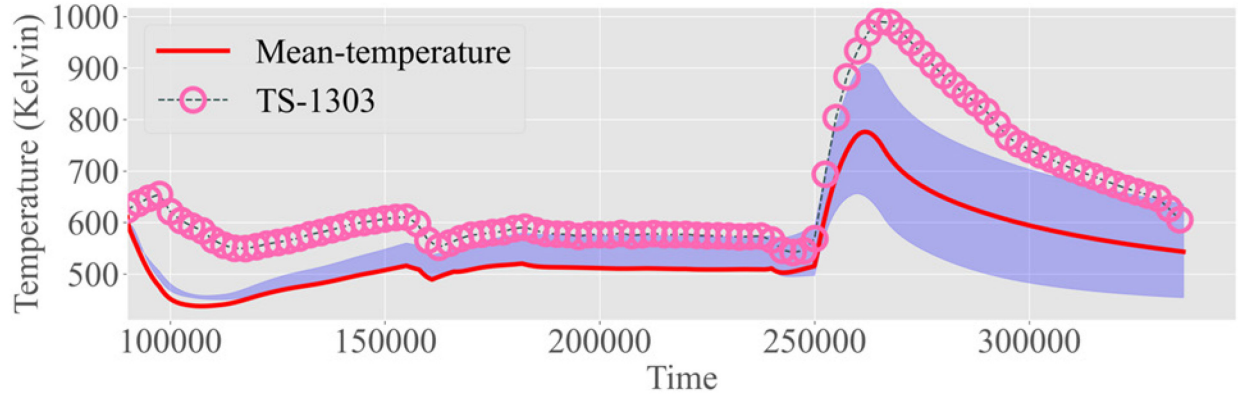


Figure 14. Statistical variation of the temperature in Core Block #3 and Pprimary Sector #5 owing to the variation in the conductivity. The bands show  $\mu \pm 2\sigma$ .

Further, all the temperature sensor readings taken from the RELAP5-3D simulation were compared with the experimental data and a distribution of them is plotted in Core Block # 3 and Block # 1 in a 2D fashion (the location of the sensor in various sectors and their angular, radial positions are shown in Tables 5 and 6). The sectors of the core blocks are marked in blue and green in Figure 15 for Core Block # 1 and in blue, green, and purple in Figure 16 for Core Block # 3.

Table 4. Sensor locations in Core Block # 1.

Sensor	Sector	Angle	Radial Location
TS-1107	Sector#1	0.0	0.0
TS-1108	Sector#1	5.45	0.18
TS-1109	Sector#1	10.90	0.33
TS-1111	Sector#1	16.36	0.36
TS-1113	Sector#1	21.81	0.47
TS-1116	Sector#1	27.27	0.27
TS-1117	Sector#1	32.72	0.52
TS-1118	Sector#1	38.18	0.67
TS-1119	Sector#1	43.63	0.67
TS-1120	Sector#1	49.09	0.67
TS-1124	Sector#2	54.54	0.36
TS-1128	Sector#2	132.0	0.6
TS-1129	Sector#2	144.0	0.27
TS-1131	Sector#2	156.0	0.67
TS-1132	Sector#2	168.0	0.67
TS-1133	Sector#2	180.0	0.67

Table 5. Sensor locations in Core Block # 3.

<b>Sensor</b>	<b>Sector</b>	<b>Angle</b>	<b>Radial Location</b>
TS-1301	Sector#1	0.0	0.0
TS-1302	Sector#1	5.45	0.18
TS-1303	Sector#1	10.90	0.33
TS-1305	Sector#1	16.36	0.36
TS-1307	Sector#1	21.81	0.38
TS-1309	Sector#1	27.27	0.6
TS-1310	Sector#1	32.72	0.85
TS-1311	Sector#1	38.18	0.27
TS-1312	Sector#1	43.63	0.52
TS-1313	Sector#1	49.09	0.67
TS-1314	Sector#1	54.54	0.67
TS-1315	Sector#1	60.0	0.67
TS-1316	Sector#2	120.0	0.18
TS-1317	Sector#2	127.5	0.33
TS-1319	Sector#2	135.0	0.36
TS-1321	Sector#2	142.5	0.47
TS-1323	Sector#2	150.0	0.6
TS-1324	Sector#2	157.5	0.52
TS-1326	Sector#2	165.0	0.85
TS-1328	Sector#2	172.5	0.67
TS-1329	Sector#2	180.0	0.67
TS-1331	Sector#3	180.0	0.33
TS-1333	Sector#3	188.57	0.36
TS-1337	Sector#3	197.14	0.6
TS-1338	Sector#3	205.71	0.85
TS-1339	Sector#3	214.28	0.27
TS-1340	Sector#3	222.85	0.52
TS-1341	Sector#3	231.42	0.67
TS-1343	Sector#3	240.0	0.67

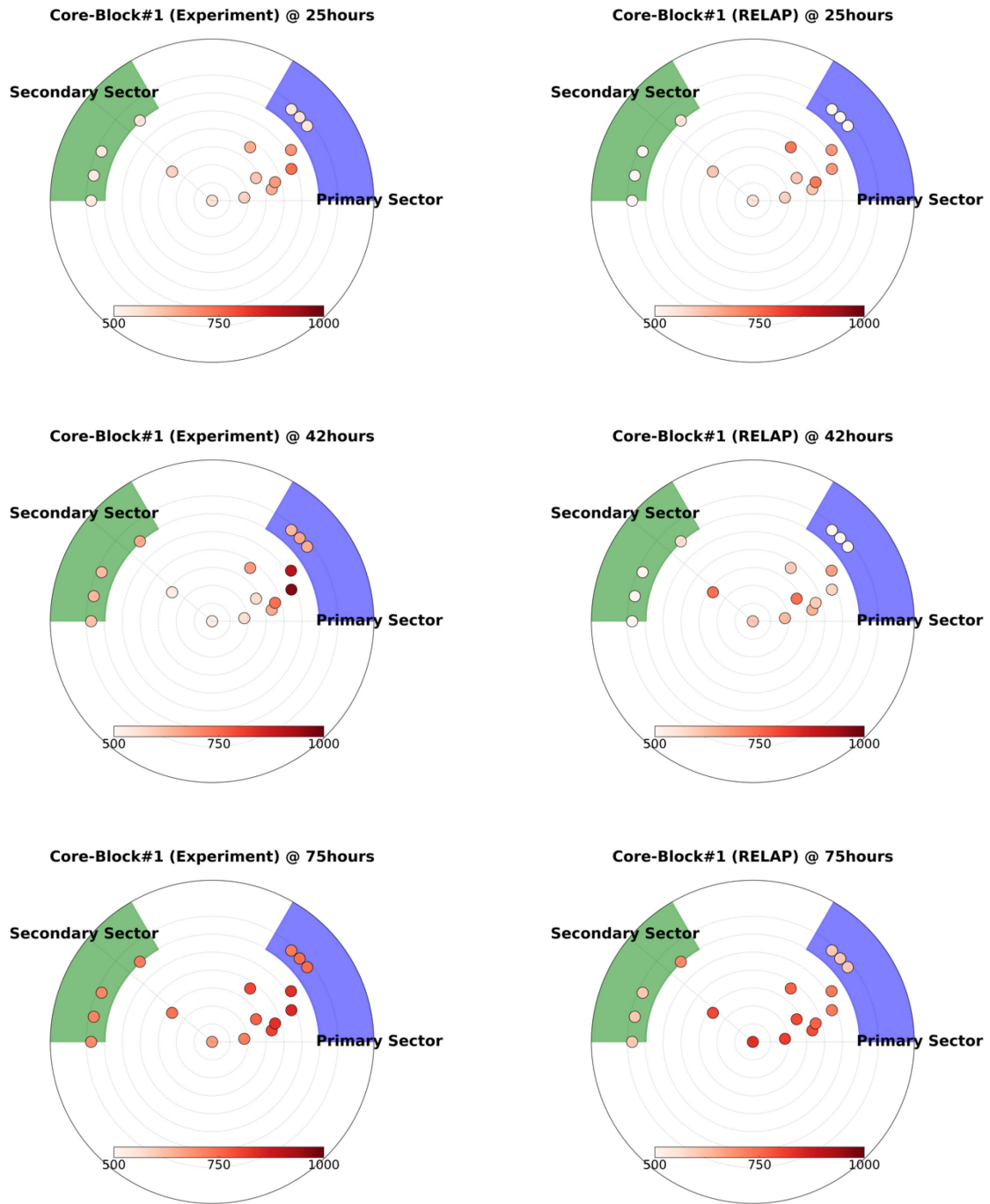


Figure 15. Temperature distribution (in Kelvin) in Core Block #1.

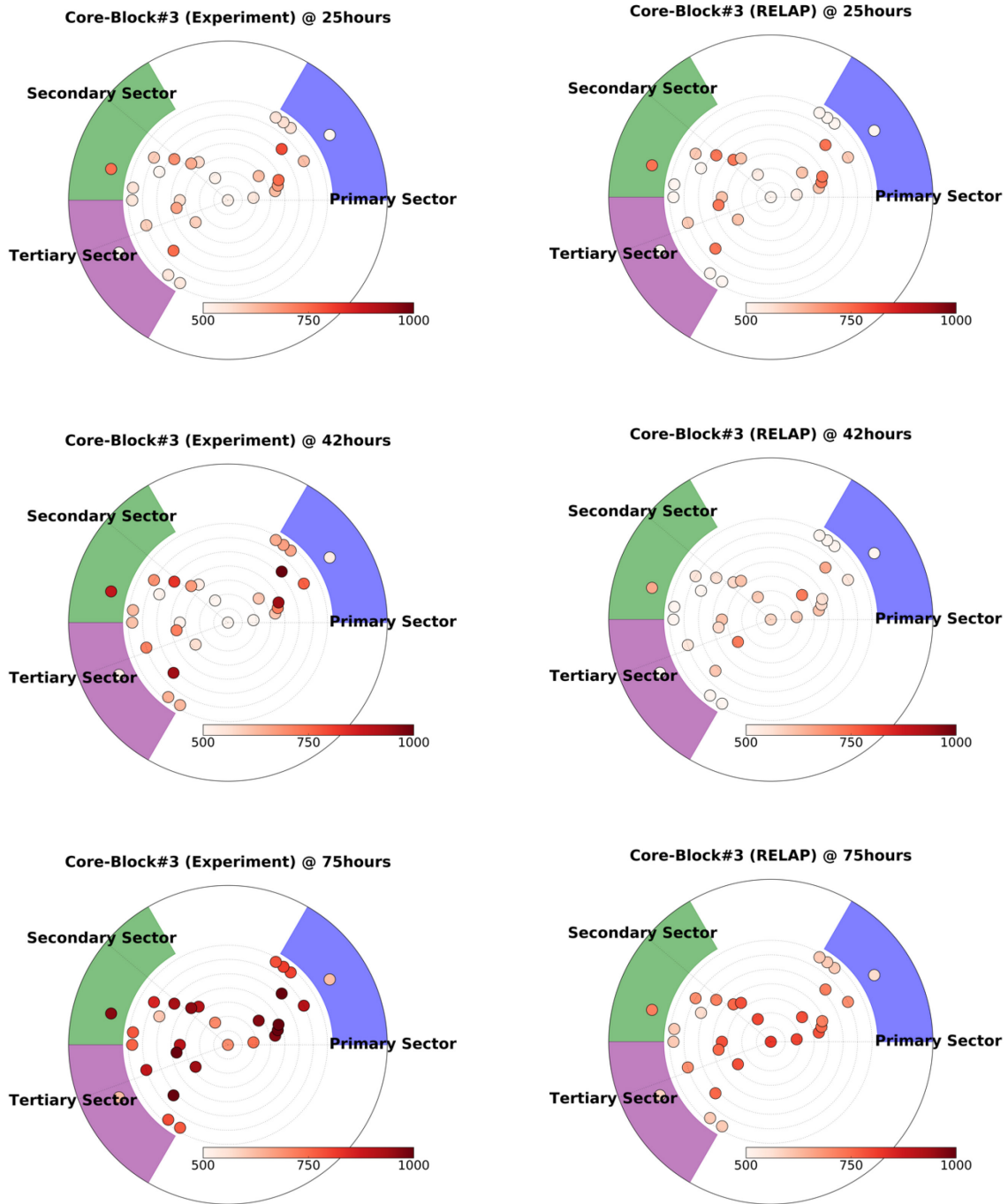


Figure 16. Temperature distribution (in Kelvin) in Core Block #3.

Figure 15 and 16 demonstrate the observed differences between the RELAP5-3D simulation and the experimental data. Though the trends are the same, the simulated values have a difference of almost 100+ kelvins in Core Block #1 while it is even more in Core Block #3.

## 6.1 Conclusion

We performed the PG-27 simulation on the RELAP5-3D 1D thermal-hydraulics code and analyzed experimental data to gather the boundary conditions for the code. The key performance metric is that the graphite temperature was compared against the experimental data. The computational model shows good overall agreement with the general data trend. Some discrepancies are obvious because of the parametric uncertainties in the model. They arise because of the two main factors; the calculation of the helium circulator mass flow rate and of the graphite conductivity. Getting the exact time-varying rate of the mass flow rate and the temperature-dependent profile of the material conductivity is an essential step to exactly match the conduction-dominant physics of the experiment. Those exact calculations are reserved for future studies and analysis.



## REFERENCES

- Bayless, Paul D. 2018. "RELAP5-3D Input Model for the High Temperature Test Facility." INL/EXT-18-45579, Idaho National Laboratory. (not published).
- Davis, Cliff. 2018. "Validation of RELAP5-3D Using HE-FUS3 Data." INL/EXT-18-46153-Rev000, Idaho National Laboratory. <https://doi.org/10.2172/1637889>.
- Epiney, Aaron S. 2020. "RELAP5-3D Modeling of High Temperature Test Facility (HTTF) Test PG-26." INL/EXT-20-59902-Rev000, Idaho National Laboratory. <https://doi.org/10.2172/1676420>.
- Mesina, George L. 2016. "A history of RELAP computer code." Nuclear Science and Engineering 5-19. <https://doi.org/10.13182/NSE16-A38253>
- Mesina, George L, David Aumiller, F.X. Buschman. 2016. "Extremely Accurate Sequential Verification of RELAP5-3D." Nuclear Science and Engineering 182: 1–12. <https://doi.org/10.13182/NSE14-151>.
- Neylan, A.J., D.V. Graf, and A.C. Millunzi. 1988. "The modular high temperature gas-cooled reactor (MHTGR) in the US." Nuclear Engineering and Design 109(1–2): 99–105. [https://doi.org/10.1016/0029-5493\(88\)90146-X](https://doi.org/10.1016/0029-5493(88)90146-X).
- Novo, Alessandro del, and Emanuela Martelli. 2016. "Validation of a Three-Dimensional Model of EBR-II and Assessment of RELAP5-3D Based on SHRT-17 Test." Nuclear Technology 193(1): 1–14. <https://doi.org/10.13182/NT14-152>.
- Uspuras, E., A. Kaliatka, and E. Bubelis. 2004. "Validation of coupled neutronic/thermal-hydraulic code RELAP5-3D for RBMK-1500 reactor analysis application." Annals of Nuclear Energy 31(15): 1667–1708. <https://doi.org/10.1016/j.anucene.2004.06.002>.
- Woods, Brian. 2019. "OSU High Temperature Test Facility Design Technical Report, Revision 2." DOE-OSU-14517-116-10244, Oregon State University. <https://www.osti.gov/biblio/1599410>.
- Woods, Brian, and Seth R. Cadell. 2019. OSU High Temperature Test Facility Test Acceptance Report PG-27 Low Power (<350kW) Complete Loss of Flow, 2 Heaters OSU-HTTF-TAR-027-R0. Corvallis: Oregon State University.